Original Article

MOLECULAR PAIN

Molecular Pain
Volume 13: 1–13

DOI: 10.1177/1744806917745179
journals.sagepub.com/home/mpx
SAGE

Characterisation of Nav1.7 functional expression in rat dorsal root ganglia neurons by using an electrical field stimulation assay

Antoine Fouillet[1], Jake F. Watson[1], Andrew D. Piekarz[2], Xiaofang Huang[2], Baolin Li[2], Birgit Priest[2], Eric Nisenbaum[2], Emanuele Sher[1] and Daniel Ursu[1]

Abstract

Background: The $Na_v1.7$ subtype of voltage-gated sodium channels is specifically expressed in sensory and sympathetic ganglia neurons where it plays an important role in the generation and transmission of information related to pain sensation. Human loss or gain-of-function mutations in the gene encoding $Na_v1.7$ channels (SCN9A) are associated with either absence of pain, as reported for congenital insensitivity to pain, or with exacerbation of pain, as reported for primary erythromelalgia and paroxysmal extreme pain disorder. Based on this important human genetic evidence, numerous drug discovery efforts are ongoing in search for Nav1.7 blockers as a novel therapeutic strategy to treat pain conditions.

Results: We are reporting here a novel approach to study $Na_v1.7$ function in cultured rat sensory neurons. We used live cell imaging combined with electrical field stimulation to evoke and record action potential-driven calcium transients in the neurons. We have shown that the tarantula venom peptide Protoxin-II, a known $Na_v1.7$ subtype selective blocker, inhibited electrical field stimulation-evoked calcium responses in dorsal root ganglia neurons with an IC_{50} of 72 nM, while it had no activity in embryonic hippocampal neurons. The results obtained in the live cell imaging assay were supported by patch-clamp studies as well as by quantitative PCR and Western blotting experiments that confirmed the presence of $Na_v1.7$ mRNA and protein in dorsal root ganglia but not in embryonic hippocampal neurons.

Conclusions: The findings presented here point to a selective effect of Protoxin-II in sensory neurons and helped to validate a new method for investigating and comparing $Na_v1.7$ pharmacology in sensory versus central nervous system neurons. This will help in the characterisation of the selectivity of novel $Na_v1.7$ modulators using native ion channels and will provide the basis for the development of higher throughput models for enabling pain-relevant phenotypic screening.

Keywords

Sodium channels, Nav1.7, protoxin-II, dorsal root ganglia neurons, electrical field stimulation, calcium imaging

Date received: 25 April 2017; revised: 14 September 2017; accepted: 28 September 2017

Background

Voltage-gated sodium (Nav1) channels are ion channels expressed in all excitable cells (neurons and muscle cells) and play a specific physiological role in the initiation and propagation of action potentials.

This large family of sodium channels consist of nine different subtypes classified based on the main alpha subunit (Nav1.1 to Nav1.9).[1] Some Nav subtypes are exclusively expressed in specific tissues, with Nav1.4 (in muscle) and Nav1.5 (in cardiac tissue) showing the highest specificity. The other Nav subtypes are present at various expression levels throughout the different parts of the central nervous system (CNS) and peripheral nervous system. Of particular interest to pain-related drug discovery are the Nav subtypes found to be primarily expressed in sensory neurons, such as Nav1.7 and

[1]Lilly Research Centre, Eli Lilly and Company, Windlesham, UK
[2]Lilly Research Laboratories, Eli Lilly and Company, IN, USA

Corresponding author:
Daniel Ursu, Lilly Research Centre, Eli Lilly and Company, Windlesham, Surrey GU20 6PH, UK.
Email: Daniel.Ursu.J@gmail.com

Nav1.8.[2,3] Their predominant expression within the pain pathway points to a direct contribution to the generation and/or maintenance of chronic pain conditions, which are most often characterised by a state of peripheral nerve hyper-excitability. Multiple studies linked mutations in the SCN9A gene (encoding Nav1.7) to inherited pain conditions. These mutations can cause either exacerbation of pain (gain-of-function mutations)[4–7] or reduction or complete lack of pain sensation (loss-of-function mutations).[8–10] Enhancement of channel function by changes in either channel activation or inactivation kinetics has been associated with erythromelalgia or paroxysmal extreme pain disorder, conditions characterised by intermittent attacks of severe pain.[7,11–13] Together, these findings make Nav1.7 an attractive target to pursue in search for novel therapeutics aimed at treating pain conditions. Indeed, multiple drug discovery efforts have been initiated by various pharmaceutical companies[14,15] aiming at finding novel molecular entities that can selectively block Nav1.7 channels. These efforts are ongoing and present themselves with multiple challenges in particular around discovering molecules with good selectivity within the Na_v channel family.

Pharmacological tools for studying sodium channels have been available for a long time, starting with the discovery of Tetrodotoxin (TTX), a toxin with high selectivity for a subset of Nav1 channels. Small molecules that selectively block sodium channels have also been discovered and are used successfully in clinical practice. Compounds like lidocaine and procaine are used as local anaesthetics mainly for blocking acute pain associated with surgery and/or dentistry interventions and also for topical treatments in chronic neuropathic pain. All of these pharmacological tools have usually very good selectivity for sodium channels over other ion channels and receptors but offer limited Nav1 subtype selectivity.[16,17] Protoxin (ProTx)-I and ProTx-II are peptides isolated from a tarantula venom and were shown to inhibit sodium channels by shifting their voltage dependence of activation to more positive potentials.[18] Subsequent studies have established that ProTx-II selectively inhibits human recombinant Nav1.7 versus the other Nav1 channels with a fold separation of about 100× between the IC_{50} values measured using the whole cell voltage-clamp technique.[19] Nav1.7 selectivity has also been reported for other peptides, either in their native form or after rational changes made to the peptide structure.[20–22] The efforts to modify and improve the properties of ProTx-II led to the improvement of selectivity versus the other Nav subtypes without overall increase in potency.[20]

Historically, various assays have been used for studying voltage-gated ion channels either in heterologous expression systems or in native tissues/neurons. Electrophysiology, in the form of whole cell voltage clamp techniques, remains the preferred method for studying ion channel function as it offers the possibility of measuring the ion channel currents directly while maintaining a very good control over the membrane potential. Alternatively, current clamp techniques are used most often when the aim is to evaluate the contribution of native sodium channel function to excitability and the generation of action potentials. Alternative methods that rely on indirect measurement of membrane potential have also been used successfully to investigate sodium channel function. Either small-molecule dyes[23–25] or genetically encoded proteins can serve as voltage sensors.[26,27] These methodologies offer great potential for enabling future high throughput optical assays for studying sodium channel function.

In this report, we present a novel approach for studying voltage-gated sodium channel function in a native neuronal environment by focusing in particular on the Nav1.7 subtype. We have used live cell imaging to measure sodium channel function indirectly by looking at action potential (AP)-induced calcium responses triggered by electrical field stimulation (EFS) in cultured primary neurons. By using subtype selective and non-selective pharmacological tools (ProTx-II and TTX), we compared specific functional responses of Nav1.7 in rat dorsal root ganglia (DRG) neurons and rat embryonic hippocampal (EH) neurons. Our results point to a selective inhibition by ProTx-II of EFS responses in DRG neurons but not in EH neurons, while TTX worked non-specifically. We have also performed mRNA and protein expression studies and confirmed the selective expression of Nav1.7 in rat DRG neurons.

Methods

Primary neuronal culture

DRG were isolated from three to five weeks male Sprague-Dawley rats by a method described previously[28] with minor modifications. Briefly, rats were killed by exposure to a rising concentration of CO_2 followed by cervical dislocation. Ganglia from all spinal levels were dissected in chilled PBS (without Ca^{2+}/Mg^{2+}, Invitrogen, Paisley, UK). All animal work was performed in accordance with the UK Animal Scientific Procedures Act of 1986, and all procedures were approved through the British Home Office Inspectorate. DRG tissues were dissociated following two different types of enzymatic digestions. DRG tissue was first incubated for 1 h with collagenase (0.125%) diluted in F12 media supplemented with 10% FBS (PAA Laboratories GmbH) and Penicillin/Streptomycin (1X-Gibco, UK) at 37°C. Tissue was washed with PBS and further digested for 10 min at 37°C with 0.25% trypsin-EDTA. Tissue was triturated

using a 1-ml Gilson pipette. DRG neurons were separated from myelin and cellular debris by centrifugation for 10 min at $145 \times g$ on top of 2 ml of F12/FBS supplemented with BSA 15%. Pellets containing DRG neurons were resuspended in 400 µl of F12/FBS. For calcium imaging experiment, 5 µl drop of cell suspension was added in the middle of the well of a Biocoat PDL 96 well-plate coated with laminin at 20 µg/ml (Sigma Aldrich, UK). Cells were left to attach to the plate for 1 to 2 h at 37°C 5% CO_2; 100 µl of F12/FBS media supplemented with 35 µg/ml uridine and 15 µg/ml 5-fluoro-2-deoxyuridine was added to the cells to block growth of glia cells. Cells were kept in culture for 7 to 10 days before performing the experiments. The addition of the mitotic inhibitors minimised the growth of glia cells and promoted good adherence of the neurons to the plastic substrate for the long-term studies (7 to 10 days in culture). In the absence of the mitotic inhibitors, the neurons will quickly (2 to 3 days) cluster together (ganglionate) and detach from the plastic surface. For patch-clamp experiments, 5 µl drop of cell suspension was added in the middle of a glass coverslip coated with PDL and laminin (NeuVitro Corporation, US), and grown as above.

Rat hippocampal tissues were dissociated from E18 embryos of pregnant Sprague-Dawley rats purchased from Charles River Laboratories (Margate, UK). Hippocampi (8–10) were dissociated in 10-ml trypsin-EDTA for 10 min at 37°C. Trypsin-EDTA solution was removed and inactivated with 5 ml neurobasal medium (Invitrogen, Paisley, UK) supplemented with 10% heat-inactivated foetal bovine serum (FBS, PAA Laboratories GmbH), B27 supplement (Life technologies, Inc) and L-glutamine (PAA Laboratories GmbH). The neurobasal medium was then replaced with 2.5 ml Hank's balanced salt solution (HBSS, Invitrogen, Paisley, UK) supplemented with 20 mg/ml DNase (Sigma-Aldrich, Poole, UK) and gently triturated with a 1-ml Gilson pipette. Once the cells were dissociated, 7.5 ml HBSS with DNAse was added and centrifuged for 5 min at 5°C and $200 \times g$ (RCF). Rat hippocampal neurons were resuspended in neurobasal media supplemented with B27 supplement (Life technologies, Inc) and L-glutamine (PAA Laboratories GmbH) and plated at 2×10^5 cells/ml into Biocoat PDL 96-well plates (100 µl/well).

For patch-clamp experiments, rat hippocampal neurons were plated at 1×10^5 cells/ml (100 µl/cover slip) on Biocoat poly-D-lysine (PDL)/laminin coverslips (NeuVitro Corporation, USA). Cells were kept in culture for 7 to 10 days before performing the experiments.

Live cell calcium imaging

Rat EH and DRG neurons were loaded with 100 µl/well of 4 µM calcium-sensitive dye Fluo4-AM in the presence of 1% pluronic acid (Invitrogen, Paisley, UK) diluted in HEPES-buffered Tyrode's solution (HBTS, Invitrogen, Paisley, UK) containing (mM): 135 NaCl, 5 KCl, 1.2 $MgCl_2$, 2.5 $CaCl_2$, 10 HEPES, 11 glucose, pH = 7.2. Cells were incubated for 60 min in the dark at room temperature. Cells were washed and subjected to EFS experiments in the presence of HBTS, drugs or toxins. Platinum–iridium electrodes (Science Products GmbH, Hofheim, Germany) were placed adjacent to the optical field (Figure 1(a)) and used to deliver voltage pulses with defined characteristics (intensity and frequency) using a stimulus generator (NPI, Tamm, Germany). The duration of the electrical stimulus was set to a fixed value of 2 ms and was kept constant in all our experiments.

The stimulation electrodes and the drug solution delivery were combined in a perfusion pencil (Figure 1(a)) that can be automatically positioned (via a linear actuator—Zaber Technologies, Vancouver, Canada) in the vertical direction at a set height above the bottom of the well of a multiwell plate. As part of the daily calibration routine of the system, the electrodes were lowered into the well until they touched the bottom of the well and then they were moved at exactly 500 µm above.

Drug solution application was made via a eight-line gravity-driven perfusion system (Automate Scientific, Berkley, CA, USA) at a flow rate of ~1.5 mL/min enabling a fast application of drug on the cells. The outflow suction tubing was adjusted at a height corresponding to a residual volume in the well of about 100 uL. This will produce the complete replacement of the well solution every 4 s. Dye-loaded cells were viewed using an inverted epifluorescence microscope (Axiovert 135TV, Zeiss, Cambridge, UK). Fluo-4 fluorescence was excited by a 480 ± 10 nm light source (Polychrome II, TILL-Photonics, Gräfelfing, Germany) and emission was captured by a iXon 897 EMCCD camera (Andor Technologies, Belfast, UK) after passing through a dichroic mirror (505LP nm) and a high-pass barrier filter (515LP nm). The light application was synchronised with the camera exposure (usually between 10 and 20 ms), so the illumination was intermittent to prevent phototoxicity. A high acquisition frame rate of 10 frames/s was used during application of the EFS pulse train while slower rates were used between stimuli (1 frame every 10 s). Digitised images were recorded and processed by using Imaging Workbench 5.0 software (INDEC Biosystems, Santa Clara, CA, USA). Regions of interest (image mask) were selected based on an automatic thresholding algorithm. Only the cells (regions) that showed a change in fluorescence following application of the first train of stimuli were quantified. This was done by subtracting the image corresponding to the baseline (10 s before stimulus application) from the image corresponding to the maximum calcium responses

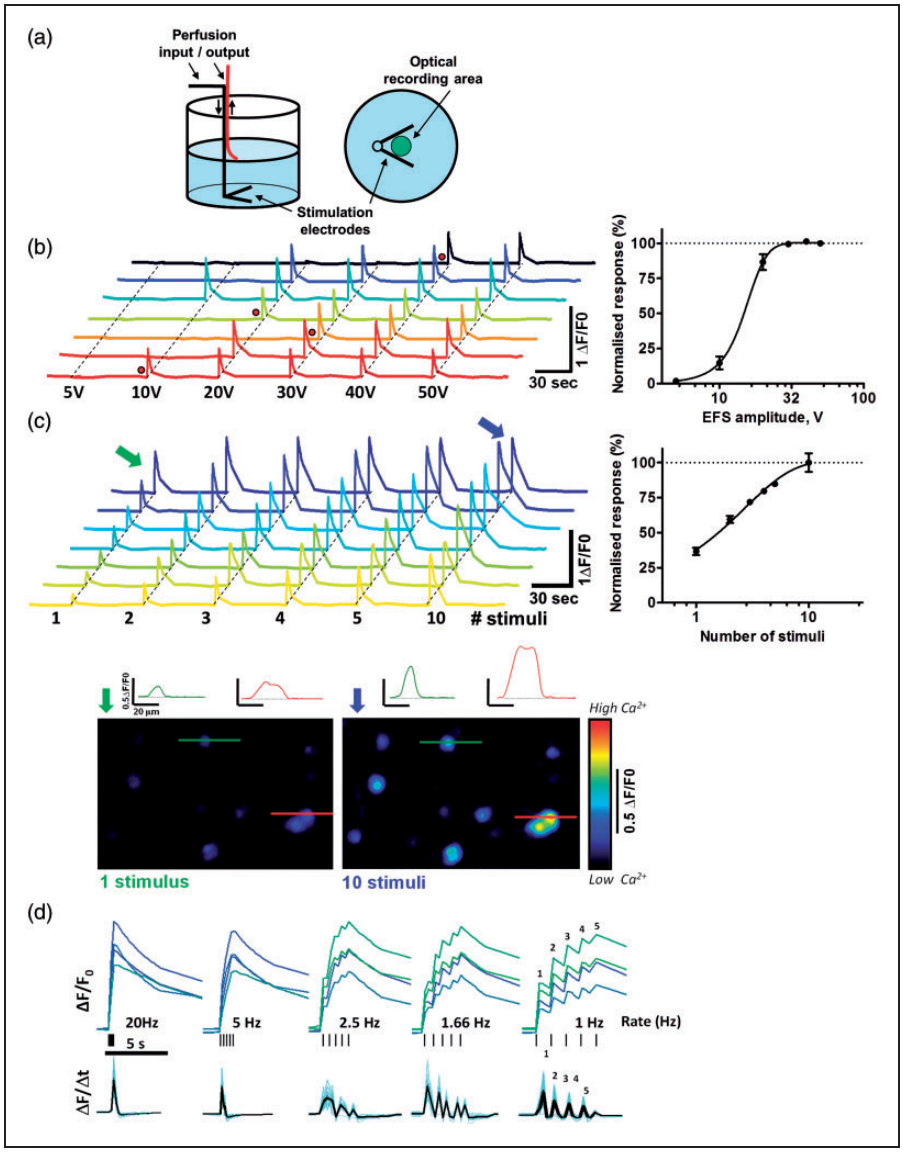

Figure 1. Electrical field stimulation triggers calcium fluxes in rat DRG neurons. (a) Schematic representation of a single well (from a 96-well plate) showing the position of the perfusion inlet/outlet and of stimulation electrodes; the two electrodes are positioned around the optical recording area situated in the middle of the well. (b) DRG neurons were subjected to a single electrical stimulus at different voltages (5, 10, 20, 30, 40 and 50 V). Each individual trace corresponds to the calcium response induced by EFS in a single neuron. The number of neurons responding to EFS stimulation increased with increasing EFS amplitude while the response magnitude remained constant. The panel on the right shows the averaged data for cells from three different wells. (c) DRG neurons showed increased response amplitude upon increasing number of EFS stimuli (1, 2, 3, 4, 5 and 10 stimuli) at constant stimulation voltage (50 V). The graph in the right panel corresponds to averaged data from three different wells. Representative pseudocolour images of DRG neurons subjected to 1 stimulus (left panel) and 10 stimuli (right panel) are shown below the traces (baseline response removed). The fluorescence levels are shown as traces for selected neurons (red and green lines, scale bars correspond to 0.5 ΔF/F0 and 20 μm). (d) Calcium response pattern follows changes in EFS frequency. At very low stimulation frequency (from 2.5 to 1 Hz), the calcium response peak induced by individual AP could be distinguished easily in the trace as opposed to higher frequency where only a single peak was observed. The traces in the lower panel in (d) correspond to first derivative transformation of the fluorescence signal above showing individual AP-induced calcium fluxes over time. At 1 Hz, the five peaks matched perfectly the train of five applied electrical stimuli.

(3 s after stimulus application). The resulting image mask was then applied to the original images to analyse the responding cells. Data were analysed by averaging individual traces (corresponding to the regions of interest) collected from a large number of cells in multiple wells of the 96-well plate. Delta F/F0 values were measured by calculating the ratio between the change in fluorescence signal intensity (delta F) and baseline fluorescence (F0).

Whole cell patch clamp

Cells were voltage clamped after 7 to 10 days in culture in the whole-cell configuration mode with an AxoPatch 200A patch-clamp amplifier (Molecular Devices, Sunnyvale, CA, USA). Pipettes were pulled from borosilicate glass (Type GC150TF-10, Harvard Apparatus, Kent, UK) using a commercial puller (Model P-87, Sutter Instruments, Novato, CA, USA) and had resistances between 2 and 10 MΩ when filled with a pipette solution containing (in mM): $MgCl_2$ 1, MgATP 4, EGTA 0.5, HEPES 10, K Gluconate 140, adjusted to pH 7.3 with CsOH. The series resistance was compensated to ~70% by using the internal circuitry of the AxoPatch amplifier. All of the recordings were performed in the same extracellular solution as used for the calcium imaging experiments (HEPES buffered Tyrode's solution), except that calcium ions were completely removed to reduce the contribution of voltage-gated calcium channels (VGCCs) to the recorded currents. Data were recorded at 10 kHz using a DA/AD interface (Digidata 1322A, Molecular Devices, Sunnyvale, CA, USA) connected to a PC. Drugs were applied using a multichannel perfusion system (Model BPS-8, Scientifica, Uckfield, UK) controlled by the same software (Clampex ver. 9, Molecular Devices, Sunnyvale, CA, USA) used for recording voltage-clamp signals.

Immunostaining

Neurons were fixed with 4% paraformaldehyde (Affymetrix, UK) for 45 min at room temperature (RT) and then permeabilised and blocked with PBS-0.1% Triton X100 containing 5% BSA for 1 h at RT. Antibodies directed against Nav1.7 (Millipore, cat#AB5390, used at 1/800 dilution) and β3-tubulin (Millipore, cat# MAB1637, used at 1/250 dilution) were diluted in PBS with 0.1% triton X100 and 0.5%BSA and added to the DRG and EH neurons overnight at 4°C. Cells were incubated with Alexa-488 anti-rabbit and Alexa-555 anti-mouse (Invitrogen, both used at a 1/1000 dilution) in PBS with 0.1% triton X100 and 0.5% BSA for 1:30 h at RT in the dark. Nuclei were counterstained with Hoechst at 10 µg/ml (Life technologies, UK). Fluorescent images were recorded on a FV1000 Olympus confocal microscope.

Western blotting

DRG and EH neurons were harvested after seven days in culture. Samples were centrifuged for 5 min at 145 × *g* and pellets were resuspended in solubilisation buffer (0.32 M Sucrose, 10 mM HEPES, 2 mM EDTA—adjusted to pH 8.0, supplemented with 50 U/mL Benzonase, Complete Protease inhibitor (Roche, UK), PhosphoSTOP (Roche, UK) and 1% Triton X-100 (Sigma, UK)). Samples were centrifuged at 260,000 × *g* for 2 h at 4°C. Pellets were resuspended in solubilisation buffer supplemented with 1% Triton X-100. Protein quantification was performed using the Bradford assay following the manufacturer's guidelines (Biorad, Watford, UK). Samples were loaded onto a 3% to 8% Tris Acetate acrylamide gel and transferred onto nitrocellulose membranes. Anti-Nav1.7 and anti-β3 tubulin antibodies used for Western blotting were the same as those used for immunocytochemistry.

Quantitative PCR

Quantitative PCR was used to measure Nav1.x expression at the mRNA level. Total RNA was isolated from cultured rat DRG and EH neurons (seven days in culture) using TRIzol reagent (Thermo Fisher Scientific/Invitrogen, Lenexa, KS) by following the manufacturer's instructions. The isolated total RNA was reversely converted to cDNA using the SuperScript III kit (Thermo Fisher Scientific, Lenexa, KS). In brief, 2 µl of total RNA (250 ng/µl) was mixed with 10 µl of 2X reaction mix, 2 µl of RT enzyme and 6 µl nuclease-free water. The reverse transcription reaction was conducted at 25°C for 10 min followed by 50°C for 30 min and 85°C for 5 min. After chilling on ice, 1 µl of RNase H was added into each reaction and the mixture was incubated at 37°C for 20 min. The cDNA was diluted four times with nuclease-free water. The qPCR reaction was performed by mixing 2.5 µl of diluted cDNA with 2 µl of nuclease-free water, 5 µl of TagMan gene expression master mix (Thermo Fisher Scientific/Applied Biosystems, Lenexa, KS) and 0.5 µl of Nav1.x primer/probe mix (Thermo Fisher Scientific/Applied Biosystems, Lenexa, KS, Hprt1, Rn01527840_m1; Scn1a, Rn00578439_m1; Scn2a, Rn00680558_m1; Scn3a, Rn01485332_m1; Scn4a, Rn01461132_m1; Scn5a, Rn00565502_m1; Scn8a, Rn00570506_m1; Scn9a, Rn00591020_m1, Scn10a, Rn00568393_m1; Scn11a, Rn00570487_m1;). The qPCR reaction was run in triplicate with Quant Studio 7 Flex with pre-set relative qPCR program. The Ct value was calculated with a fixed threshold at 0.2 for all targets. ΔCt was calculated as $\Delta Ct = Ctgene - CtHprt$. Data presented in graphs are relative expression to Hprt1, expressed as ΔΔCt ($\Delta\Delta Ct = \Delta Ct_{gene} - \Delta Ct_{normaliser\ (Hprt1)}$).

Data analysis and statistics

Mean data are plotted as mean ± S.E.M. (n = number of experiments). To obtain IC_{50} values, concentration response data were fitted to a four-parameter logistic model using GraphPad Prism. IC_{50} values are presented as mean and 95% confidence intervals. Student's

two-sided t-test was used to test for significant differences of mean values (assuming two independent populations; $p = 0.05$ unless otherwise stated).

Compounds

TTX was purchased from Tocris (Bristol, UK) and ProTx-II from PeptaNova (Sandhausen, Germany). Stocks were prepared in distilled water and stored in the freezer (−20°C) until used for experiments.

Results

EFS induces calcium transients in cultured rat DRG neurons

In order to study activation of sodium channels in cultured neurons, we developed a method to assess neuronal excitability by indirectly monitoring single cell calcium transients elicited by EFS. The system was designed to allow for automatic sequential recordings in a multiwell plate (96 well plate format) combined with perfusion of drug solutions and application of EFS (Figure 1(a)). The perfusion pencil that allows for controlled perfusion (inflow and outflow) of the well content can be moved automatically between wells and contains a pair of field electrodes that can deliver custom pulse protocols produced by a stimulus generator. Neurons located in the region adjacent to the two electrodes were subjected to EFS (Figure 1(a) – right panel). Initially, we aimed to determine the relation between the stimulus properties (amplitude, number and frequency) and calcium response in DRG neurons. Application of single stimuli with increased amplitude (Figure 1(b)) revealed the characteristic all-or-nothing response for individual neurons. The example traces presented in Figure 1(b) also show that different neurons in the same recording field had different thresholds for eliciting responses. While the amplitude of the calcium transient did not change with increasing stimulus amplitude, more neurons were recruited to the point that at amplitudes higher than 40 V, all the neurons in the field were responding. The average data recorded from multiple wells ($n = 3$ wells) are plotted in the right panel graph in Figure 1(b).

The amplitude of the calcium transients increased with application of multiple stimuli (Figure 1(c)). In this case, a constant supramaximal stimulus amplitude was used (50 V) while varying the number of stimuli from 1 to 10. Representative single cell calcium responses are shown in Figure 1(c) with average data from $n = 3$ wells plotted in the right panel graph. The pseudocolour images of DRG neurons in Figure 1(c) illustrate the spatial distribution of the individual neuronal responses at the peak of the calcium transient for the conditions where 1 or 10 stimuli were applied (green and blue arrows on the example trace graph). The increase in calcium response amplitude upon application of multiple electrical stimuli is associated with the fast kinetics of calcium entry through VGCCs, accumulation of calcium in the neuron and relatively slow rate of removal of intracellular calcium ions.

Finally, the effect of changing the frequency of EFS on calcium flux kinetics was also investigated (Figure 1(d)). When stimulating at 20 Hz (5 stimuli), the recorded calcium responses showed a kinetic with only a single peak being measured by the system. At low frequency of stimulation (1 Hz, 5 stimuli), calcium fluxes followed precisely the pattern of stimulation allowing us to discriminate the individual responses, corresponding to single APs, elicited by each electrical pulse. Similar patterns of calcium responses were observed for the other intermediate stimulation frequencies. A further analysis of the calcium flux kinetics, by calculating the first derivative of the signal (dF/dt) offers a better view on the individual responses and represents a way to separate and easily analyse responses elicited by single stimuli.

EFS-evoked calcium responses are blocked by a selective sodium channel blocker

To demonstrate that sodium channels are directly involved in the generation of the EFS-induced calcium responses, we evaluated the activity of a classical sodium-channel blocker, TTX (Figure 2). Neurons were first subjected to a control EFS pulse train (5 stimuli, 50 V) followed by a second identical EFS train (test EFS) in the presence or absence of the channel blocker. The reproducibility of the evoked calcium response following two consecutive EFS was determined in the absence of drug (correlation plot in Figure 2(a)). The amplitude of the individual neuronal responses to the test EFS was plotted against the amplitude to the control EFS and showed a strong correlation ($R^2 = 0.77$, $p < 0.0001$), suggesting minimal run down obtained with this stimulation paradigm. By using this protocol, a concentration response curve for TTX was determined on both DRG (Figure 2(b) and (c)) and EH neurons (Figure 2(d)).

Representative traces of DRG neurons subjected to EFS in the presence of TTX (1 nM, 10 nM and 100 nM) are shown in Figure 2(b). Increasing concentration of TTX resulted in increased block of the calcium response, yielding an IC_{50} value of 11.0 nM (7.1 to 17.0 nM, $n = 4$ experiments) (Figure 2(c)). Even at the highest tested TTX concentration (300 nM), some responses were not blocked by the application of TTX, probably due to expression of TTX-insensitive sodium channels. A concentration-response curve for TTX was also determined in EH neurons and yielded an IC_{50} value

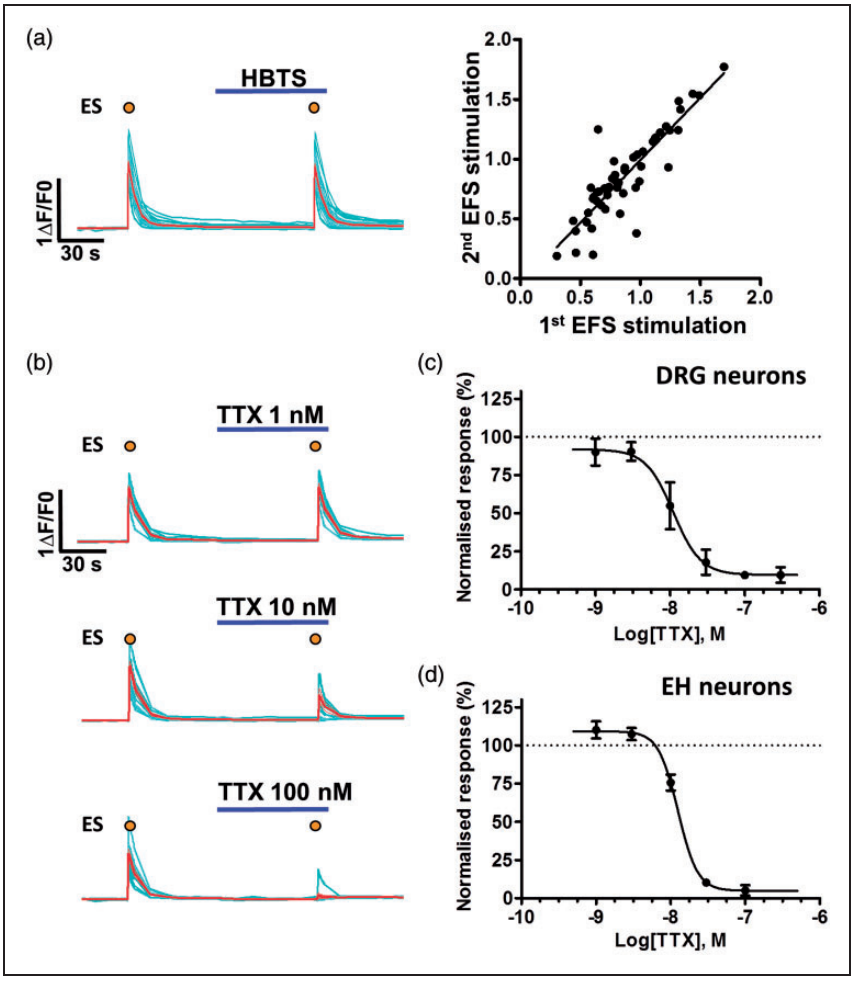

Figure 2. Sodium channels are involved in the generation of EFS-evoked calcium fluxes in DRG and hippocampal neurons. (a) A double stimulation protocol (5 stimuli, 50 V) was used to study sequential EFS calcium responses in DRG and hippocampal neurons. Correlation plot ($R^2 = 0.77$, $p < 0.001$) between the first and second EFS response in DRG neurons to demonstrate very good reproducibility in the amplitude of the measured responses (data from 3 wells, n = 49 cells). (b) Representative examples of calcium responses induced by EFS in DRG neurons subjected to Tetrodotoxin (TTX) at 1, 10 nM and 100 nM. (c and d) Concentration response curves of TTX on EFS induced calcium fluxes in DRG and hippocampal neurons. (c) TTX blocked DRG and hippocampal neurons calcium fluxes in a dose dependent manner. IC_{50} values were 11.0 nM (7.1 to 17.0 nM, n = 4) for DRG neurons and 12.5 nM (10.3 to 15.3, n = 3) for hippocampal neurons.

of 12.5 nM (10.3 to 15.3, n = 3) (Figure 2(d)). These data confirm the direct involvement of sodium channels in the generation of APs upon EFS, recorded here as an increase in intracellular calcium concentration.

Nav1.7 channels are involved in generation of EFS-evoked calcium transients in rat DRG neurons

Using the single cell calcium imaging assay, we then evaluated whether voltage-gated Nav1.7 channels are involved in the generation of the EFS-evoked calcium responses. ProTx-II, a tarantula venom peptide that has been shown to preferentially block Nav1.7 over other Nav1.x subtypes,[19] was evaluated in the EFS calcium imaging assay on both the DRG and the EH neurons (Figure 3). Representative individual neuronal responses to EFS (blue traces) and averaged responses of all the neurons (red traces) are shown in Figure 3(a) and (b) for DRG and EH neurons (for control, 100 nM and 300 nM ProTx-II), respectively. We have changed the EFS protocol for this experiment to allow for a longer incubation period with ProTx-II and also by testing for responses after 1 min and 5 min of drug incubation. As we observed that responses at time 1 min were only partially blocked by ProTx-II, only the responses recorded following 5 min incubation with ProTx-II were used for further analysis.

Although responses were completely blocked by ProTx-II (300 nM) in most DRG neurons, there were a few neurons which still appeared to generate APs, probably corresponding to neurons expressing Nav1.8 and/or Nav1.9. In EH neurons, ProTx-II did not affect the

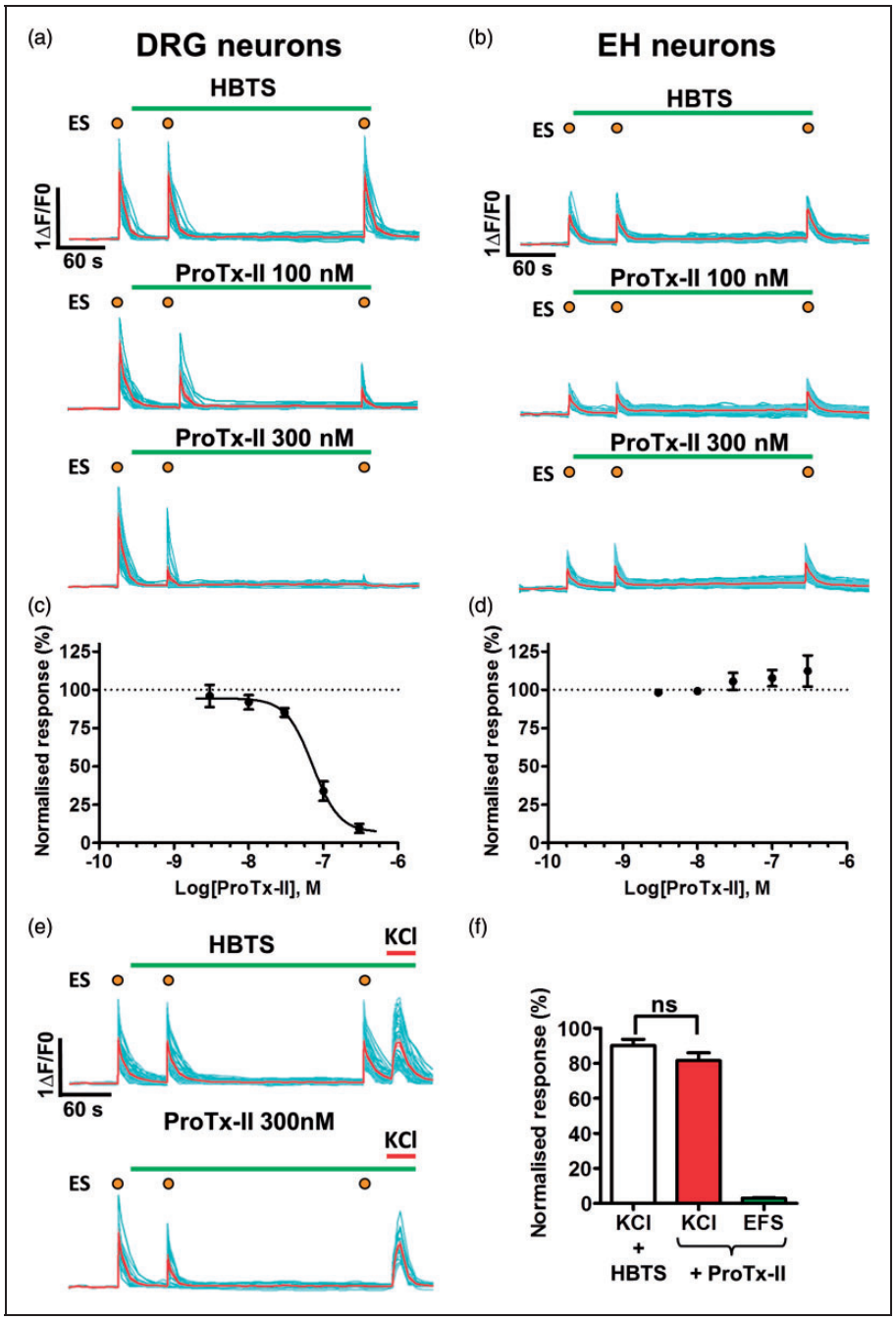

Figure 3. ProTx-II blocks EFS-evoked calcium fluxes in rat DRG neurons but has no effect in rat hippocampal neurons. Representative single cell recordings for DRG (a) and hippocampal (b) neurons are shown from experiments following incubation with different concentrations (control, 100 nM and 300 nM) of ProTx-II. Nearly complete block of EFS-evoked calcium responses was observed following perfusion for 5 min with 300 nM ProTx-II in DRG neurons (a), while the same concentration of ProTx-II had no effect on calcium transients in hippocampal neurons (b). Concentration response curves for ProTx-II in DRG neurons (c) and hippocampal neurons (d) are also shown. IC_{50} value was 72 nM (54 to 96, n = 4) for DRG neurons. (e). ProTx-II did not block voltage-gated calcium channels in DRG neurons. Effect of ProTx-II on KCl-induced calcium transients in DRG neurons. ProTx-II (300 nM) fully blocked EFS-induced calcium fluxes but did not affect responses elicited by 35 mM KCl. (f) Averaged data (normalised to first EFS stimulation in each well) from three independent wells for the experiment shown in (e).

generation of APs. The concentration response curves for ProTx-II are shown in Figure 3(c) and (d) for DRG and EH neurons, respectively. While we could observe a clear dose dependent block by ProTx-II in DRG neurons with IC_{50}= 72 nM (54 to 96, n = 4), there was a lack of activity on EH neurons where no block could be observed even at the highest ProTx-II concentration (300 nM). We have also confirmed that the effect observed with ProTx-II was not due to an unspecific block of VGCCs (Figure 3(e) and (f)). In this experiment, VGCCs were activated directly by membrane depolarisation following perfusion with a 35-mM KCl containing buffer. Since ProTx-II caused no inhibition on KCl-induced calcium fluxes, it is unlikely that the effect of ProTx-II on EFS-evoked calcium responses was caused by block of calcium channels selectively expressed by DRG neurons.

To confirm the findings from the single cell calcium imaging assay, the whole cell patch clamp technique was used to assess the effect of ProTx-II on sodium currents in both DRG and EH neurons. Sodium currents were recorded every 10 s by application of voltage steps from a holding potential of −80 mV to −20 mV for a duration of 25 ms and combined with perfusion of toxin containing extracellular solutions. Representative sodium current traces are shown in Figure 4(a) for all four different conditions tested (DRG and EH neurons, with or without 100 nM TTX or 300 nM ProTx-II). Only the first 4 ms of the current trace is shown to illustrate the effect of toxins on the Nav current peak. Application of TTX (100 nM) almost completely abolished the peak sodium currents in both DRG (9.3 ± 4.9% remaining, n = 6) and EH neurons (7.3 ± 3.8% remaining, n = 3) (Figure 4(a) and (b)). Application of ProTx-II on DRG significantly reduced sodium channel current levels to 11.9 ± 2.9% (n = 6) as compared to EH neurons where only a partial effect was observed (63.8% ± 3.0, n = 3, $p < 0.001$). These data are in close agreement with our calcium imaging data where ProTx-II blocked AP-induced calcium fluxes in DRG but not in EH neurons.

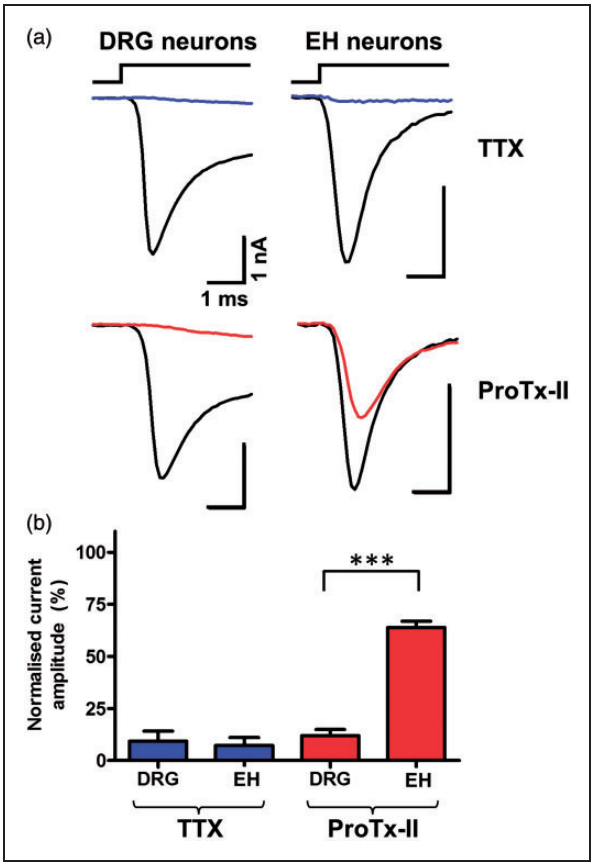

Figure 4. ProTx-II blocks sodium channel currents in DRG neurons. (a) Whole cell patch-clamp recordings in DRG and hippocampal neurons were performed to investigate the effect of TTX and ProTx-II on sodium currents (elicited by a test voltage step of 25 ms duration from −80 mV holding potential to −20 mV). Representative sodium current traces from DRG and hippocampal neurons are shown before (black line) and after application of 100 nM TTX (top panel, blue trace) and 300 nM ProTx-II (bottom panel, red trace) for a total duration of 5 min. (b) Averaged data for the experiment in (a) showing normalised amplitude of sodium currents in DRG and hippocampal neurons after incubation with ProTx-II (300 nM) and TTX (100 nM); n = 3–6 cells, ***$p < 0.001$.

Nav1.7 is the major sodium channel subtype expressed in rat DRG neurons

To support the observed differential pharmacological effects of ProTx-II on DRG and EH neurons, we performed a comparative study to look at both the protein and mRNA expression of Nav1.7 in the two neuronal preparations used in this study. A quantitative PCR technique was used to evaluate mRNA levels for all Nav1.x channel subtypes (Figure 5(a)). Based on relatively high mRNA expression, Nav1.1, 1.2, 1.3 and 1.6 appear to be the most abundant sodium channel subtypes expressed in the rat EH neurons. The DRG neurons mainly expressed Nav1.7 with much lower values determined for Nav1.8 and Nav1.3 (Figure 5(a)).

The data shown here point to a completely different pattern of expression of the sodium channel subtypes, with a clear lack of expression of Nav1.7 in EH neurons and a relative high expression in DRG neurons. To demonstrate that the differential mRNA expression of Nav1.7 translates to similar difference in protein levels, immunostaining and Western blotting experiments were carried out (Figure 5(b) and (c)). Dual staining for Nav1.7 and β3-tubulin showed clear staining for Nav1.7 in DRG neurons in the soma and processes (Figure 5(b) – white arrows) but not in the hippocampal neurons. The finding was confirmed using the Western

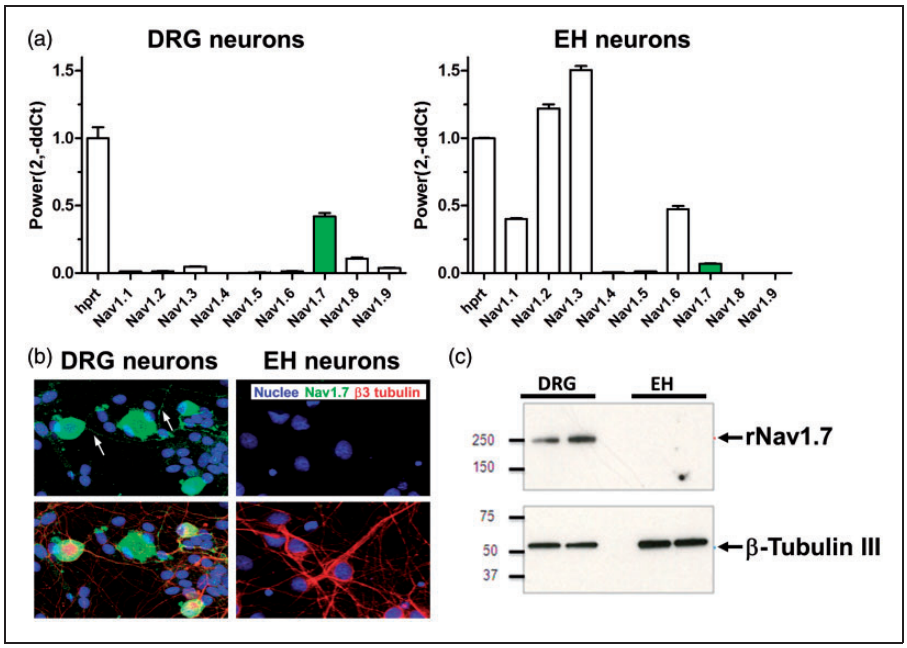

Figure 5. Expression of Nav1.7 channels in DRG and hippocampal neurons. (a) Relative mRNA expression for all Nav1.x subtypes was assessed in both neuronal preparations by QPCR. Expression levels of Nav1.x alpha subunits are shown relative to Hprt1 gene. Nav1.7 was detected only in DRG neurons but not in hippocampal neurons. (b) Expression of Nav1.7 channels in DRG and hippocampal neurons was also assessed by immunocytochemistry with antibodies against Nav1.7 (green), β3-tubulin (red) and nuclei (Hoechst - blue). Top panels show the overlap of Nav1.7 staining and Hoechst to highlight the Nav1.7-specific staining in soma and processes in DRG neurons but not in hippocampal neurons. Bottom panels include also the specific neuronal staining of β3-tubulin. (c) Nav1.7 channels protein expression in DRG and hippocampal neurons was evaluated by Western blotting; β3-tubulin was used as loading control. Nav1.7 expression was only observed in DRG neurons with a band at ~230KDa but not in hippocampal neurons.

blot technique which also showed the presence of Nav1.7 protein in DRG neurons but not in hippocampal neurons (Figure 5(c)).

Discussion

We aimed in this study to establish and validate a simple method to investigate sodium channel function, in particular of the Nav1.7 subtype, in sensory neurons as an in vitro model to evaluate novel Nav1.7 modulators in a native neuronal environment.

The two preparations that we have chosen for our study are known to express different subtypes of voltage-gated sodium channels.[29–32] In full agreement with the literature, we confirmed that under our specific experimental conditions, Nav1.7 expression is relatively high in DRG neurons, both at mRNA and protein levels, but it is completely absent in the EH neurons. Nav1.1, Nav1.2, Nav1.3 and Nav1.6 are the Nav subtypes expressed at high levels in the EH neurons. We should note however that the DRG neurons we are using in this study are isolated from juvenile animals while the hippocampal neurons are of embryonic origin. This might explain the high levels of Nav1.3 expression in EH neurons (see Shah et al.[31]).

We have used the above two neuronal preparations in the past for studying the pharmacology of ligand-gated ion channels: either for TRPV1 receptors[28,33] or nicotinic Acetylcholine receptors.[34] We modified and adapted the methods used previously for studying ligand-gated ion channels, which relied on recording calcium responses following application of selective agonists. For studying voltage-gated ion channels, in particular for investigating Nav channels, we modified the system to allow application of EFSs to trigger generation of APs and secondary calcium transients. We first thoroughly characterised the basic properties and effects of different EFS parameters by establishing relationships between EFS intensity, frequency and number of stimuli and calcium response amplitude. We then demonstrated, by using a selective Nav channel blocker (TTX), that EFS-evoked calcium transients are triggered by Nav channel activation. The data obtained from these initial experiments demonstrate clearly the direct involvement of Nav channels in generation of the calcium responses in the neuronal preparations used under our experimental conditions.

By using the above methodology, we evaluated the activity of ProTx-II and showed that it blocked the EFS responses in DRG neurons. In a similar concentration range (up to 300 nM), ProTx-II showed

no inhibition of EFS-induced calcium transients in the other EH neurons. We therefore conclude that the main voltage-gated sodium channel subtype contributing to EFS-evoked calcium transients in cultured rat DRG neurons is Nav1.7. This conclusion is supported by the results from the patch clamp experiments performed with ProTx-II and TTX in the two neuronal preparations. ProTx-II fully inhibited sodium currents in DRG neurons but had only partial effects on currents recorded in EH neurons. The partial block observed with ProTx-II in EH neurons (~36% inhibition at 300 nM ProTx-II) did not translate in block of EFS-evoked responses. It could be that there is a minimum block of current (i.e., >40% necessary to inhibit APs and correspondingly the EFS-evoked responses). For a specific amplitude and duration of the electrical stimulus, one would need to block that amount of sodium current that will prevent the change in membrane potential to reach the threshold for generating an action potential. It does not appear that we have reached that level of block at 300 nM ProTx. Considering that the steepness of the concentration response curves for both TTX and ProTx are high (2.4 and 3.3 for TTX in DRG and EH neurons, respectively, and 2.4 for ProTx-II in DRG neurons), we can assume that APs inhibition (like the AP generation) is also an all-or-none phenomenon.

As far as we are aware, this is the first study to show a clear pharmacological separation of the effects of ProTx-II in a peripheral neuronal preparation (sensory neurons) versus a central nervous system neuronal preparation (hippocampal neurons). A previous study showed a specific block by ProTx-II of C-fiber-evoked APs in an isolated nerve preparation.[19] There is however an apparent disconnect in this study between the reported potency of ProTx-II on recombinant human Nav1.7 (0.1 nM) compared to potency determined in the native preparation (IC_{50}~1 μM). Potential explanations for this discrepancy include reduced access of the toxin to the ion channels on the axons (though the study used a desheathed nerve preparation) and also structural differences between the recombinant and native channels. In our DRG neuronal culture, the potency of ProTx-II for blocking EFS responses ($IC_{50} = 71$ nM) falls somewhere between the value obtained in recombinant Nav1.7 channels and the isolated nerve preparation reported by Schmalhofer et al.[19] study.

The assay we describe in this study is highly relevant for investigating sodium channel function because it evaluates the physiological function of native sodium channels, i.e., the generation of APs, under conditions that preserve the intracellular environment. One limitation of the model presented here is that it relies on recording sodium channel function indirectly by measuring changes in intracellular calcium levels following activation of VGCCs. However, this can also be seen as an advantage of the assay because it can provide valuable information on cross-reactivity of the tested compounds on VGCCs. By performing parallel measurements using a different mode of activation of VGCCs (i.e., by KCl-induced depolarisation), one can exclude compounds with poor Nav selectivity.

The strategy we have followed in the present study is applicable for investigating the comparative activity of novel Nav1.7 inhibitors at peripheral sensory neurons and CNS neurons. The profile of an ideal Nav1.7 selective compound should show optimum activity on blocking DRG neuron responses while being inactive in the hippocampal neurons, similar to what we have shown here for ProTx-II. The assay format presented here allows for automated, medium throughput evaluation of compound activity, the only limitation in terms of scalability being the limited number of DRG neurons obtained during acute isolations from adult animals. One advantage of a calcium flux assay is the possibility of transfer to a high-throughput platform, several of which are readily available in the drug discovery environment (FLIPR®, Molecular Devices, USA; FDSS®, Hamamatsu, Japan; Mantra®, Galenea, USA). Some of these systems have already been adapted to implement EFS protocols (FDSS® and Mantra®).

We have previously used the calcium flux EFS assay for demonstrating cellular excitability of human-induced pluripotent stem cell-derived neurons and modulation by standard sodium channel blockers.[35] The strategy presented here for rat primary neurons can be further expanded to a similar comparative study of human Nav1.7 native channels by performing the assay in induced pluripotent stem cells differentiated into CNS subtypes (cortical forebrain neurons) versus peripheral nervous system subtypes (sensory neurons) which are readily available.[36–39] This would open up the potential for implementing high-throughput assays for screening directly on human-cultured neurons and eventually speed up the drug discovery process for the identification of novel selective sodium channel blockers.

In summary, we describe here a new approach for studying Nav1.7 channel function and pharmacology in rodent cultured neurons. The novelty of the method resides in the combination of EFS with measurement of APs-induced calcium transients for investigating Nav1.7 channels in an enriched Nav1.7 neuronal population (DRG neurons). We have validated the technique by using specific Nav channel blockers and custom-designed EFS protocols. Based on the observed selective block by ProTx-II and on the Nav channel subtype expression pattern, we found that Nav1.7 channels are the major Nav subtype involved in generation of the EFS-evoked responses in DRG neurons. The method presented here can be of great use for the development of novel selective Nav1.7 blockers and confirmation

of activity in a native neuronal preparation (sensory neurons) and for evaluating their selectivity versus Nav subtypes expressed in the central nervous system (e.g., in hippocampal neurons).

Acknowledgments

The authors gratefully acknowledge the contributions of Jeremy Findlay and Elizabeth Folly for primary cell culture support.

Authors' contributions

AF and DU performed the calcium imaging studies, JW performed the patch-clamp study, AF performed the ICC, ADP performed the Western blotting and XH and BL performed the mRNA expression studies. DU supervised the studies and their planning and drafted the manuscript. All authors read, edited and approved the final manuscript.

Declaration of Conflicting Interests

The author(s) declared the following potential conflicts of interest with respect to the research, authorship, and/or publication of this article: All the authors are employed by Eli Lilly and Company.

Funding

The author(s) received no financial support for the research, authorship, and/or publication of this article.

References

1. Catterall WA. Voltage-gated sodium channels at 60: structure, function and pathophysiology. *J Physiol* 2012; 590: 2577–2589.
2. Bagal SK, Marron BE, Owen RM, et al. Voltage gated sodium channels as drug discovery targets. *Channels (Austin)* 2015; 9: 360–366.
3. Emery EC, Luiz AP and Wood JN. Nav1.7 and other voltage-gated sodium channels as drug targets for pain relief. *Expert Opin Ther Targets* 2016; 20: 975–983.
4. Yang Y, Wang Y, Li S, et al. Mutations in SCN9A, encoding a sodium channel alpha subunit, in patients with primary erythermalgia. *J Med Genet* 2004; 41: 171–174.
5. Han C, Rush AM, Dib-Hajj SD, et al. Sporadic onset of erythermalgia: a gain-of-function mutation in Nav1.7. *Ann Neurol* 2006; 59: 553–558.
6. Dib-Hajj SD, Cummins TR, Black JA, et al. From genes to pain: Na v 1.7 and human pain disorders. *Trends Neurosci* 2007; 30: 555–563.
7. Fertleman CR, Baker MD, Parker KA, et al. SCN9A mutations in paroxysmal extreme pain disorder: allelic variants underlie distinct channel defects and phenotypes. *Neuron* 2006; 52: 767–774.
8. Cox JJ, Reimann F, Nicholas AK, et al. An SCN9A channelopathy causes congenital inability to experience pain. *Nature* 2006; 444: 894–898.
9. Ahmad S, Dahllund L, Eriksson AB, et al. A stop codon mutation in SCN9A causes lack of pain sensation. *Hum Mol Genet* 2007; 16: 2114–2121.
10. Goldberg YP, MacFarlane J, MacDonald ML, et al. Loss-of-function mutations in the Nav1.7 gene underlie congenital indifference to pain in multiple human populations. *Clin Genet* 2007; 71: 311–319.
11. Tang Z, Chen Z, Tang B, et al. Primary erythromelalgia: a review. *Orphanet J Rare Dis* 2015; 10: 127.
12. Estacion M, Dib-Hajj SD, Benke PJ, et al. NaV1.7 gain-of-function mutations as a continuum: A1632E displays physiological changes associated with erythromelalgia and paroxysmal extreme pain disorder mutations and produces symptoms of both disorders. *J Neurosci* 2008; 28: 11079–11088.
13. Jarecki BW, Sheets PL, Jackson JO, et al. Paroxysmal extreme pain disorder mutations within the D3/S4-S5 linker of Nav1.7 cause moderate destabilization of fast inactivation. *J Physiol* 2008; 586: 4137–4153.
14. Sun S, Cohen CJ and Dehnhardt CM. Inhibitors of voltage-gated sodium channel Nav1.7: patent applications since 2010. *Pharm Pat Anal* 2014; 3: 509–521.
15. King GF and Vetter I. No gain, no pain: NaV1.7 as an analgesic target. *ACS Chem Neurosci* 2014; 5: 749–751.
16. Catterall WA and Swanson TM. Structural basis for pharmacology of voltage-gated sodium and calcium channels. *Mol Pharmacol* 2015; 88: 141–150.
17. de Lera RM and Kraus RL. Voltage-gated sodium channels: structure, function, pharmacology, and clinical indications. *J Med Chem* 2015; 58: 7093–7118.
18. Priest BT, Blumenthal KM, Smith JJ, et al. ProTx-I and ProTx-II: gating modifiers of voltage-gated sodium channels. *Toxicon* 2007; 49: 194–201.
19. Schmalhofer WA, Calhoun J, Burrows R, et al. ProTx-II, a selective inhibitor of NaV1.7 sodium channels, blocks action potential propagation in nociceptors. *Mol Pharmacol* 2008; 74: 1476–1484.
20. Flinspach M, Xu Q, Piekarz AD, et al. Insensitivity to pain induced by a potent selective closed-state Nav1.7 inhibitor. *Sci Rep* 2017; 7: 39662.
21. Rahnama S, Deuis JR, Cardoso FC, et al. The structure, dynamics and selectivity profile of a NaV1.7 potency-optimised huwentoxin-IV variant. *PLoS One* 2017; 12: e0173551.
22. Deuis JR, Wingerd JS, Winter Z, et al. Analgesic effects of GpTx-1, PF-04856264 and CNV1014802 in a mouse model of NaV1.7-mediated pain. *Toxins (Basel)* 2016; 8: E78.
23. Fromherz P, Hubener G, Kuhn B, et al. ANNINE-6plus, a voltage-sensitive dye with good solubility, strong membrane binding and high sensitivity. *Eur Biophys J* 2008; 37: 509–514.
24. Grenier V, Walker AS and Miller EW. A small-molecule photoactivatable optical sensor of transmembrane potential. *J Am Chem Soc* 2015; 137: 10894–10897.
25. Huang CJ, Harootunian A, Maher MP, et al. Characterization of voltage-gated sodium-channel blockers by electrical stimulation and fluorescence detection of membrane potential. *Nat Biotechnol* 2006; 24: 439–446.
26. Kralj JM, Douglass AD, Hochbaum DR, et al. Optical recording of action potentials in mammalian neurons using a microbial rhodopsin. *Nat Methods* 2011; 9: 90–95.

27. St-Pierre F, Marshall JD, Yang Y, et al. High-fidelity optical reporting of neuronal electrical activity with an ultrafast fluorescent voltage sensor. *Nat Neurosci* 2014; 17: 884–889.
28. Comunanza V, Carbone E, Marcantoni A, et al. Calcium-dependent inhibition of T-type calcium channels by TRPV1 activation in rat sensory neurons. *Pflugers Arch* 2011; 462: 709–722.
29. Fukuoka T and Noguchi K. Comparative study of voltage-gated sodium channel alpha-subunits in non-overlapping four neuronal populations in the rat dorsal root ganglion. *Neurosci Res* 2011; 70: 164–171.
30. Ho C and O'Leary ME. Single-cell analysis of sodium channel expression in dorsal root ganglion neurons. *Mol Cell Neurosci* 2011; 46: 159–166.
31. Shah BS, Stevens EB, Pinnock RD, et al. Developmental expression of the novel voltage-gated sodium channel auxiliary subunit beta3, in rat CNS. *J Physiol* 2001; 534: 763–776.
32. Mechaly I, Scamps F, Chabbert C, et al. Molecular diversity of voltage-gated sodium channel alpha subunits expressed in neuronal and non-neuronal excitable cells. *Neuroscience* 2005; 130: 389–396.
33. Ursu D, Knopp K, Beattie RE, et al. Pungency of TRPV1 agonists is directly correlated with kinetics of receptor activation and lipophilicity. *Eur J Pharmacol* 2010; 641: 114–122.
34. Gill JK, Chatzidaki A, Ursu D, et al. Contrasting properties of alpha7-selective orthosteric and allosteric agonists examined on native nicotinic acetylcholine receptors. *PLoS One* 2013; 8: e55047.
35. Dage JL, Colvin EM, Fouillet A, et al. Pharmacological characterisation of ligand- and voltage-gated ion channels expressed in human iPSC-derived forebrain neurons. *Psychopharmacology (Berl)* 2014; 231: 1105–1124.
36. Wainger BJ, Buttermore ED, Oliveira JT, et al. Modeling pain in vitro using nociceptor neurons reprogrammed from fibroblasts. *Nat Neurosci* 2015; 18: 17–24.
37. Young GT, Gutteridge A, Fox H, et al. Characterizing human stem cell-derived sensory neurons at the single-cell level reveals their ion channel expression and utility in pain research. *Mol Ther* 2014; 22: 1530–1543.
38. Cao L, McDonnell A, Nitzsche A, et al. Pharmacological reversal of a pain phenotype in iPSC-derived sensory neurons and patients with inherited erythromelalgia. *Sci Transl Med* 2016; 8: 335ra56.
39. Boisvert EM, Engle SJ, Hallowell SE, et al. The specification and maturation of nociceptive neurons from human embryonic stem cells. *Sci Rep* 2015; 5: 16821.